pH Wave-Front Propagation in the Urea-Urease Reaction

Magdalena M. Wrobel,[†] Tamás Bánsági, Jr.,[†] Stephen K. Scott,[†] Annette F. Taylor,[†*] Chris O. Bounds,[‡] Arturo Carranza,[‡] and John A. Pojman[‡]

[†]School of Chemistry, University of Leeds, Leeds, United Kingdom; and [‡]Department of Chemistry, Louisiana State University, Baton Rouge, Louisiana

ABSTRACT The urease-catalyzed hydrolysis of urea displays feedback that results in a switch from acid (pH ~3) to base (pH ~9) after a controllable period of time (from 10 to >5000 s). Here we show that the spatially distributed reaction can support pH wave fronts propagating with a speed of the order of 0.1–1 mm min^{-1}. The experimental results were reproduced qualitatively in reaction-diffusion simulations including a Michaelis-Menten expression for the urease reaction with a bell-shaped rate-pH dependence. However, this model fails to predict that at lower enzyme concentrations, the unstirred reaction does not always support fronts when the well-stirred reaction still rapidly switches to high pH.

INTRODUCTION

Feedback is ubiquitous in biology and drives behaviors such as biochemical switches (a large-amplitude transition between states) and rhythms (1). Combining the production of an autocatalytic species with diffusion in a spatially distributed system results in a mechanism of intercellular communication in systems such as bacteria (2), yeast (3), and the slime mold *Dictyostelium discoideum* (4). In certain cases, the spontaneous development of spatial chemical patterns during cellular morphogenesis may also be attributed to kinetic feedback coupled with transport processes (5,6).

Acid- or base-driven feedback may play an important role in biological systems. Small-amplitude pH oscillations often accompany feedback in various processes (e.g., glycolysis) and are associated with growth bursts in plants and regulation of muscle motion in microorganisms (7–9). The bacteria *Helicobacter pylori*, which is associated with stomach ulcers, uses the base-producing properties of the urea-urease reaction to protect itself against the harsh acidic environment of the stomach (10). The pH change that accompanies the reaction of urea with urease is also employed as a test for the bacteria in biosensors, and may be exploited in enzyme-based logic gates in biofuel cells (11).

Researchers have shown much interest in investigating biochemical oscillators in vitro to characterize the underlying kinetic mechanisms that give rise to nonlinear behavior (12). Methods have been developed for the design of feedback in chemical and biological systems (13,14). However, there have been relatively few studies of simple, single-phase systems in which an enzyme drives the feedback, and even fewer investigations of in vitro biochemical waves and patterns (15). An early investigation focused on NADH and proton waves in yeast cell extracts (16). Fronts have also been observed in the hydrogenase-catalyzed oxidation of hydrogen (17) and with glucose oxidase (18). These systems have complicated kinetics involving multiple enzyme states.

Almost 40 years ago, investigators proposed a feedback mechanism exploiting the bell-shaped rate-pH properties of enzymes: if the reaction produces acid and the initial pH is adjusted to a higher pH than at the maximum rate, then rate acceleration can be achieved as the reaction progresses (19,20). In simulations of ester hydrolysis by membrane-bound papain, pH waves were observed. However, experimental attempts to generate feedback by this mechanism were widely unsuccessful (21). Recently, we demonstrated that the urease-catalyzed hydrolysis of urea can show feedback driven by base (NH_3) production, resulting in a pH switch from 3 to 9 under nonbuffered conditions (22). The results were reproduced in a Michaelis-Menten model with a bell-shaped, rate-pH curve, making it possibly the simplest example of feedback in an enzyme-catalyzed reaction. The reaction is thus a good candidate for investigation of waves and pattern formation driven by biochemical feedback.

Here we show that under certain conditions, the spatially distributed urea-urease reaction supports propagating pH wave fronts that convert a mixture from acid (pH 3) ahead of the front to base (pH 9) behind. The unstirred switch time is longer than the well-stirred switch time, and at lower enzyme concentrations, the unstirred system predominantly fails to support fronts even though the well-stirred system still shows a rapid switch to high pH. The fronts are reproduced in a simple model of the reaction with the bell-shaped rate pH curve for enzyme activity and diffusion of basic reaction products NH_3 or HCO_3^-. However, this model fails to predict the stirring effects and the stochastic nature of the pH switch/fronts at low enzyme concentrations. Although it is well known that mixing can influence autocatalytic reactions, to our knowledge, the complete loss of activity in unstirred systems has not yet been reported (23). The results may have implications regarding the conditions required for

Submitted April 19, 2012, and accepted for publication June 14, 2012.

*Correspondence: a.f.taylor@leeds.ac.uk

Editor: Richard Bertram.

0006-3495/12/08/0610/6 $2.00

http://dx.doi.org/10.1016/j.bpj.2012.06.020

the reaction to induce pH changes in the bacteria *H. pylori* or in biosensors.

MATERIALS AND METHODS

We performed two types of experiments to study the urea-urease system. The temporal behavior of the system was investigated in a well-stirred batch reactor (Fig. 1 *a*), whereas its spatiotemporal dynamics was examined in a quasi-two-dimensional (quasi-2D) layer (Fig. 1 *b*). The former assembly consisted of a water-jacketed glass container of 3.8 cm diameter and 6.0 cm height in which the reaction mixture was continuously stirred at 600 rpm with a 1.5-cm-long magnetic stir bar by a magnetic stirrer (IKA-Werke, Staufen, Germany). The latter arrangement was achieved by air-tightly sandwiching a small amount of the reaction media between the upside-down lid and the base of a 5-cm-diameter petri dish (2) that was kept inside a thermostated glass dish (1) for temperature control.

The batch experiments were monitored with a pH combination electrode (Hanna HI-1131 connected to a pH meter Hanna HI-120; Hanna Instruments, Woonsocket, RI) immersed in the solution. A charge-coupled device camera and MATLAB (The MathWorks, Natick, MA) program were used to record and process images of the quasi-2D system. To visualize the sudden change in the concentration of hydrogen ions, we used the pH indicator cresol red with $pK_a = 8.3$ (Fisher Scientific, Hampton, NH). Experiments were carried out at 20°C. Typical results for both arrangements are shown in Fig. 1, *c* and *d*.

Stock solutions were prepared from ultrapure urea (National Diagnostics, Hessle, UK), urease (type III Jack beans U1500-100KU; Sigma Aldrich, St. Louis, MO), and concentrated sulfuric acid (AnalR BDH). The enzyme units quoted are determined from the average urease activity (20,990 U/g). The pH meter was calibrated with standard solutions of pH = 7.01 and pH = 4.01 (Acros Organics, Geel, Belgium) before each experimental run. The batch and 2D experiments were usually carried out in parallel to enable direct comparison. We prepared the reaction mixtures by first adding the requisite amounts of the reactant stock solutions and distilled water into the batch reactor. After stirring the system for 30 s, we removed 1.5 ml of aliquot and transferred it to an upside-down lid of a petri dish. We then carefully placed the base over the solution inside the lid, with the solution sandwiched in a thin layer between the two, at a calculated (constant) layer depth of 0.8 mm. In the final step, the petri dish assembly was placed inside the thermostated dish, which was subsequently covered.

The pH was recorded once every 10 s in the batch, and the switch time (also referred to as the clock time or induction period) was determined from the maximum of the slope of the pH-time plot. Meanwhile, snapshots were acquired of the quasi-2D system at a frame rate of 12 per minute. For mixtures with a switch time of <1000 s, fronts were allowed to spontaneously develop, whereas for those with longer reaction times, the fronts were initiated with a drop of product solution through a 1-mm-diameter hole in the center of the petri dish lid. In other pH front experiments, acid or base was used to initiate fronts; however, we found that if the pH of this solution was higher than that of the reacted solution, the diffusion of this chemical could obscure the reaction front.

The position of a moving front was determined as the inflection point on the green channel intensity profile of each RGB snapshot along a line taken in the direction of propagation. The front velocity was calculated as the slope of a straight line fitted to the series of front positions. The number of front positions available for the calculation was determined, at the given frame rate, by the time elapsed until the system switched or the fronts collided, and therefore it greatly varied between experiments. At long switch times (>1000 s), we could typically use 50–70 points (over 10 mm) for the linear fitting. When the switch time was short, we were often limited to ~12 front positions (2 mm), which resulted in increased uncertainty in the front velocities in that regime.

For each front, we determined the speed along 16 evenly spaced rays extending out from the center. In systems with a short switch time, where we relied on self-initiation, often as many as four fronts were considered in the calculation of the velocity per experiment. For reaction mixtures having a switch time of >1000 s, only the speed of the externally initiated front was taken into account. We averaged velocities from at least five experiments for each composition chosen in the urea-urease sulfuric-acid parameter space and determined the standard deviation over all experiments.

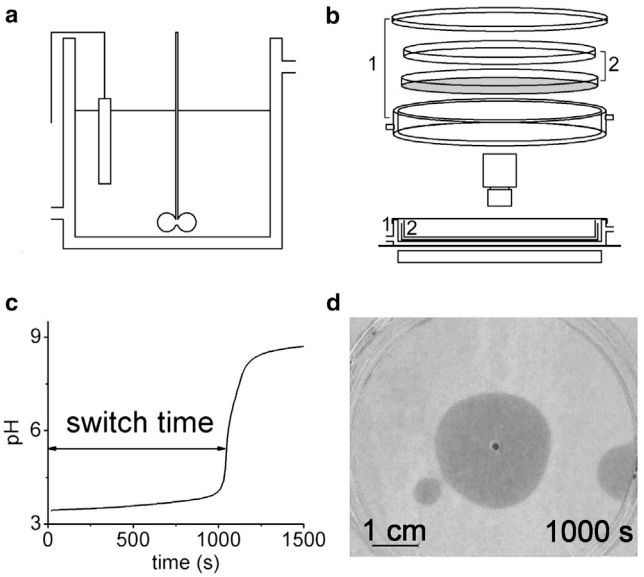

FIGURE 1 Experimental setup. (*a*) The well-stirred batch reactor apparatus with pH probe and stirrer. (*b*) Spatial apparatus with camera, where 1 indicates the outer thermostated glass dish, and 2 indicates the inner petri dish containing the reaction solution. (*c*) pH profile for $[\text{urea}]_0 = 0.023$ M, $[\text{sulfuric acid}]_0 = 4.1 \times 10^{-4}$ M, $[\text{urease}]_0 = 17$ U/ml. (*d*) pH fronts (dark = pH ~9, light = pH ~3) for the same conditions in panel *c*.

Model and simulations

The following reaction steps were taken into account:

$$\text{R1. } CO(NH_2)_2 + H_2O \xrightarrow{urease} 2NH_3 + CO_2$$
$$\text{R2. } NH_4^+ \rightleftharpoons NH_3 + H^+ \qquad pK_a = 9.25$$
$$\text{R3. } CO_2 + H_2O \rightleftharpoons H^+ + HCO_3^- \qquad pK_a = 6.35$$
$$\text{R4. } HCO_3^- \rightleftharpoons CO_3^{2-} + H^+ \qquad pK_a = 10.25.$$
$$\text{R5. } H_2O \rightleftharpoons H^+ + OH^-$$
$$\text{R6. } HSO_4^- \rightleftharpoons SO_4^{2-} + H^+$$

The rate v of the enzyme catalyzed reaction is of the Michaelis-Menten form (incorporating substrate inhibition, product inhibition, and pH dependence (24,25)):

$$v = \frac{k_1 E_T U}{\left(K_M + U\left(1 + \frac{U}{K_U}\right)\right)\left(1 + \frac{[NH_4^+]}{K_P}\right)\left(1 + \frac{K_{es2}}{[H^+]} + \frac{[H^+]}{K_{es1}}\right)}, \quad (1)$$

where E_T is the total concentration of urease in U/ml, $U = [\text{urea}]$, K_M is the Michaelis constant, K_u is the equilibrium constant for uncompetitive substrate inhibition, and K_p is the equilibrium constant for noncompetitive product inhibition. The pH dependence arises from the formation of an

active protonated form of the enzyme-substrate complex (K_{es2}) and inactive biprotonated form (K_{es1}). The enzyme parameters were within the ranges quoted in the literature (25,26), with values taken to best match the experimental results in the nonbuffered reaction: $k_1 = 2.2 \times 10^{-6}$ unit^{-1} ml M^{-1} s^{-1}; $K_M = 3 \times 10^{-3}$ M; $K_{es1} = 5 \times 10^{-6}$ M; $K_{es2} = 2 \times 10^{-9}$ M; $K_u = 3$ M; and $K_p = 2 \times 10^{-3}$ M.

The following rate constants for the reversible reactions (R2–R6) were taken from the literature (27): $k_2 = 24$ s^{-1}; $k_{-2} = 4.3 \times 10^{10}$ M^{-1} s^{-1}; $k_3 = 0.037$ s^{-1}; $k_{-3} = 7.9 \times 10^4$ M^{-1} s^{-1}; $k_4 = 2.8$ s^{-1}; $k_{-4} = 5 \times 10^{10}$ M^{-1} s^{-1}; $k_5 = 1 \times 10^{-3}$ M s^{-1}; $k_{-5} = 1 \times 10^{11}$ M^{-1} s^{-1}; $k_6 = 1.2 \times 10^9$ s^{-1}; and $k_{-6} = 1 \times 10^{11}$ M^{-1} s^{-1}.

Reactions R1–R6 resulted in a 10-variable model (H_2O is constant) with equations for the concentrations of the i^{th} variable (C_i) of the form:

$$\frac{\partial C_i}{\partial t} = f(C_i) + D_i \frac{\partial^2 C_i}{\partial x^2}, \qquad (2)$$

where $f(C_i)$ is the reaction term, D is the diffusion coefficient of C_i, and x is space. The partial differential equations associated with the spatially distributed (1D) system were solved using the package XPPaut (28) with the integration method CVODE for time and a second-order central difference approximation for diffusion terms with spatial step size $r = 0.2$ mm with the total length of the domain = 38 mm (numerical parameters: tol = 1e-14, atol = 1e-14, bandup = 10, bandlo = 10). The diffusion coefficients were taken as $D_{H+} = 5 \times 10^{-3}$ mm^2 s^{-1}; $D_{OH-} = 2 \times 10^{-3}$ mm^2 s^{-1}; and for the rest of the species $D_{Ci} = 1 \times 10^{-3}$ mm^2 s^{-1}. To initiate a front, the first two grid points were set with the concentrations of the (reacted) solution at $t = 4000$ s (C[1..2] = $C_{t=4000}$), whereas the rest of the grid points were set with the initial concentrations (C[3..190] = $C_{t=0}$). No flux boundary conditions (C[0] = C[1]; C[191] = C[190]) were used. The well-stirred zero-dimensional (0D) reaction was simulated by solving the resulting ordinary differential equations with CVODE.

RESULTS

Propagating wave fronts, converting the mixture from pH ~3 to pH ~9, were obtained for a variety of initial concentrations. Typical results are shown in Fig. 2. For setups with long switch times, the front that initiated at the center of the dish dominated the reaction domain as time progressed; however, some spontaneous initiations were observed, usually from the edges of the petri dish (Fig. 2, *a–c*). The number of spontaneous initiations increased with decreasing switch time (Fig. 2, *d–i*), and as the reaction approached the switch time, a darkening of the whole medium was observed. In most cases, the reaction time in the unstirred system was much longer than that of the well-stirred system.

The fronts propagated with constant concentration profile, as illustrated in the space-time plot in Fig. 3 *a* and the intensity-space in Fig. 3 *b*. Typical front positions in time and their corresponding linear fits for the conditions in Fig. 2 are shown in Fig. 3 *c*. Fronts were also observed in separate experiments with an open-air interface and in deeper layers of ≥ 2 mm, but deformations of the expanding circular fronts were observed. It is likely that the wave fronts were subject to convective effects under these conditions, driven by reaction-driven density differences between the product solution and reactant solution (29).

The pH fronts were reproduced in simulations of the model, with examples shown in Fig. 4 for two different

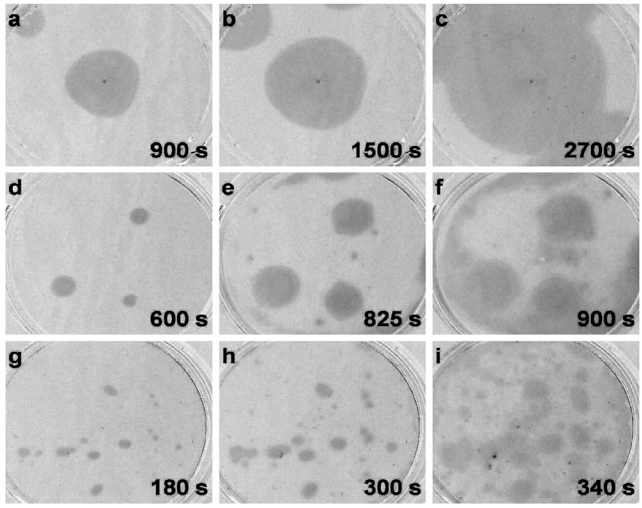

FIGURE 2 pH wave fronts (dark = pH > 9, light = pH < 4) in the urea-urease reaction for (*a–c*) $[urea]_0 = 0.009$ M, $[urease]_0 = 17$ unit/ml, $[sulfuric\ acid]_0 = 4.05 \times 10^{-4}$ M, switch time = 3000 s; (*d–f*) $[urea]_0 = 0.03$ M, $[urease]_0 = 17$ unit/ml, $[sulfuric\ acid]_0 = 4.05 \times 10^{-4}$ M, clock time = 900 s; and (*g–i*) $[urea]_0 = 0.03$ M, $[urease]_0 = 24$ unit/ml, $[sulfuric\ acid]_0 = 4.05 \times 10^{-4}$ M, clock time = 300 s. The time stamp corresponds to image time + 100 s for mixing and transfer to the petri dish.

enzyme concentrations. The pH switch in the well-stirred case is from 3 to 9, with reaction times of ~800 s and 1400 s, respectively, for these concentrations. Front propagation proceeds until the whole medium switches in pH at the same time as the well-stirred case (observed as the vertical dark band at 800 s in part ii). Propagation is driven by diffusion of the basic products: fronts are observed with diffusion of NH_3 or HCO_3^- alone (i.e., D of all other species = 0). The sharpness of the front profile is maintained during propagation (Fig. 4 *c*); however, the pH ahead of the front slowly increases as the reaction progresses. Thus, there is an acceleration of the front in time. This process is enhanced by the relatively fast diffusion of H^+ and is greatly reduced if $D_{H+} = 0$. The acceleration is more pronounced in simulations with shorter reaction times,

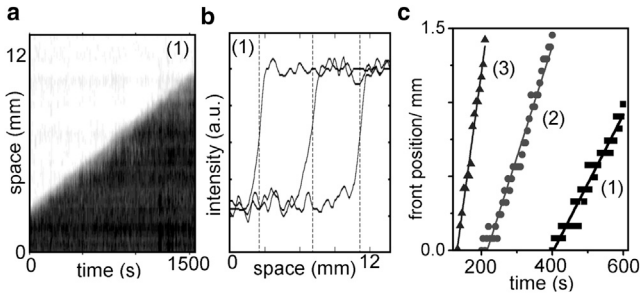

FIGURE 3 Front analysis. (*a*) Space-time plot, (*b*) profiles in space, and (*c*) front positions in time for 1), $[urea]_0 = 0.009$ M, $[urease]_0 = 17$ unit/ml, $[sulfuric\ acid]_0 = 4.05 \times 10^{-4}$ M; 2), $[urea]_0 = 0.03$ M, $[urease]_0 = 17$ unit/ml, $[sulfuric\ acid]_0 = 4.05 \times 10^{-4}$ M; and 3), $[urea]_0 = 0.03$ M, $[urease]_0 = 24$ unit/ml, $[sulfuric\ acid]_0 = 4.05 \times 10^{-4}$ M.

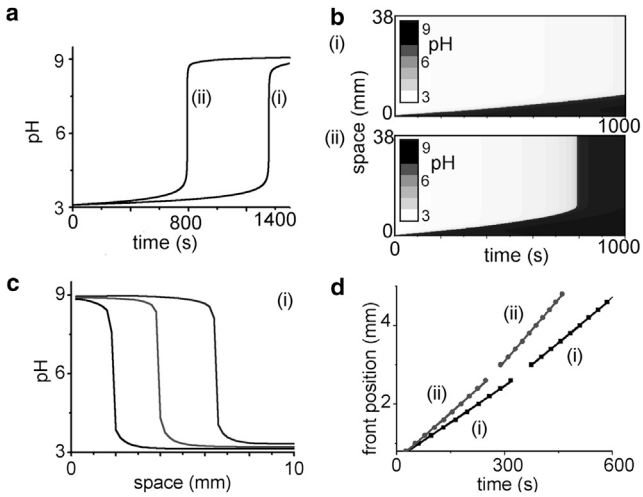

FIGURE 4 Model results for $[\text{urea}]_0 = 0.03$ M, $[\text{sulfuric acid}]_0 = 4.1 \times 10^{-4}$ M and (*i*) $[\text{urease}]_0 = 14$ U/ml and (*ii*) $[\text{urease}]_0 = 24$ U/ml. (*a*) pH-time plots in the well-stirred (0D) reaction. (*b*) Space-time plots in the 1D spatial reaction. (*c*) pH-space profiles at 200, 500, and 800 s for (*i*). (*d*) Front position in time with linear fit from 1 to 3 mm and separate linear fit from 3 to 5 mm for (*i*) and (*ii*).

and the front position in time still gives a good linear fit (with correlation coefficients > 0.998) over tens of millimeters in the case of long reaction times.

The front speed in the simulations was calculated from the slope of a linear fit of the space-time plot from 1 to 3 mm and a separate linear fit from 3 to 5 mm (Fig. 4 *d*), giving a lower and upper wave speed to compare with the experimental results (Fig. 5). The dependence of the front speeds on the initial concentrations showed the same trends in simulations and experiments, i.e., they increased with increasing urea and urease, and decreased with sulfuric acid. Thus, the front speed decreases with increasing switch time as shown in Fig. 5 *d*. A power law of the form $y = Ax^B$ was fit to the data (the fits are not shown in the figure) and resulted in values of $B = -0.481 \pm 0.001$ in simulations (*lower curve*) and $B = -0.37 \pm 0.04$ in experiments.

The relationship between front speed and switch time breaks down at lower enzyme concentrations. With the enzyme concentration reduced to 3.4 U/ml, the initial acid can also be reduced to obtain a short switch in the well-stirred batch reaction (Fig. 6 *a*). However, in the example shown in Fig. 6, the spatially distributed reaction failed to support fronts, with the drop of reacted solution at the center simply spreading diffusively (Fig. 6, *b–d*), and the medium did not switch to high pH, even when left overnight. With eight repetitions of the experiment, only one run led to front propagation and a switch to high pH. Using the enzyme concentrations employed in our earlier work (0.7–1.4 U/ml), fronts were never obtained in the unstirred medium for all the runs tried, and occasionally, for enzyme concentrations of 0.7 U/ml, the switch to high pH was sometimes not even observed in the well-stirred case.

In the spatial simulations, however, a front was always obtained for low enzyme concentrations, and the medium still switched to high pH at the same time as that predicted by the well-stirred simulation. With the same concentrations as in Fig. 6, the switch time was 800 s and the front speed was of the order of 0.55 mm min^{-1} (Fig. 7 *i*). Even with a clock time of 30,000 s for a lower enzyme concentration of

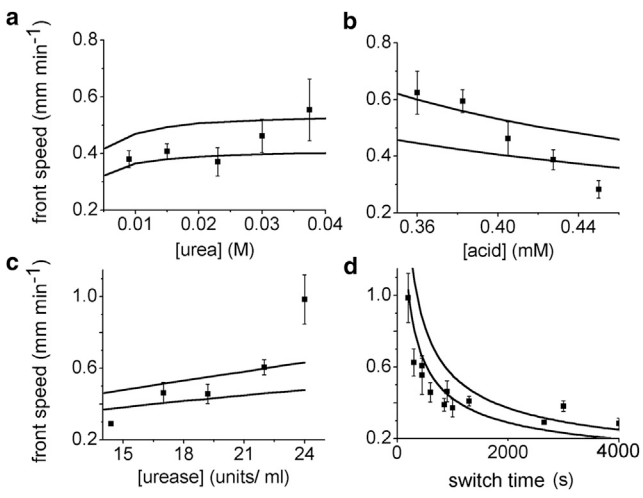

FIGURE 5 Simulated front speed (*lower line* calculated from 1 to 3 mm, *upper line* calculated from 3 to 5 mm), and experimental front speed (*squares*, error bars are standard deviations over multiple experiments) as a function of (*a*) urea, (*b*) sulfuric acid, (*c*) urease, and (*d*) switch time (calculated from well-stirred conditions). Concentrations: $[\text{urea}]_0 = 0.03$ M, $[\text{sulfuric acid}]_0 = 4.1 \times 10^{-4}$ M, and $[\text{urease}]_0 = 17$ U/ml (except when varied).

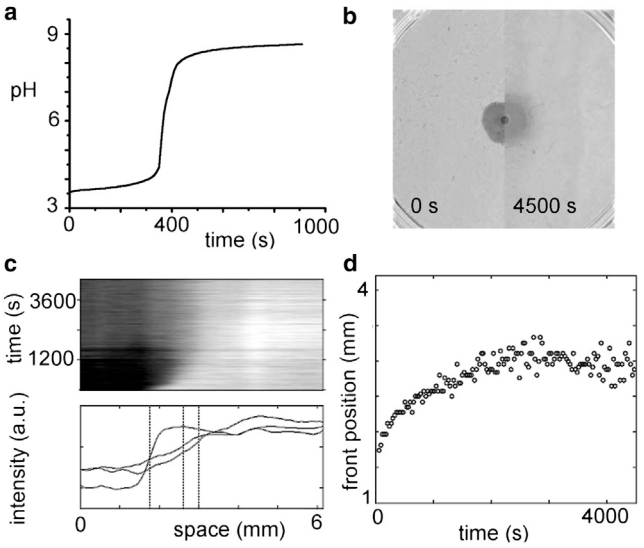

FIGURE 6 Experimental results for low enzyme: $[\text{urease}]_0 = 3.4$ unit/ ml, $[\text{urea}]_0 = 0.03$ M, and $[\text{sulfuric acid}]_0 = 1.6 \times 10^{-4}$ M. (*a*) pH-time plot in the well-stirred reaction. (*b*) Spatial reaction with reacted solution added in the center at 0 s and at 4500 s. (*c*) Space-time plot and intensity profiles. (*d*) Front position in time.

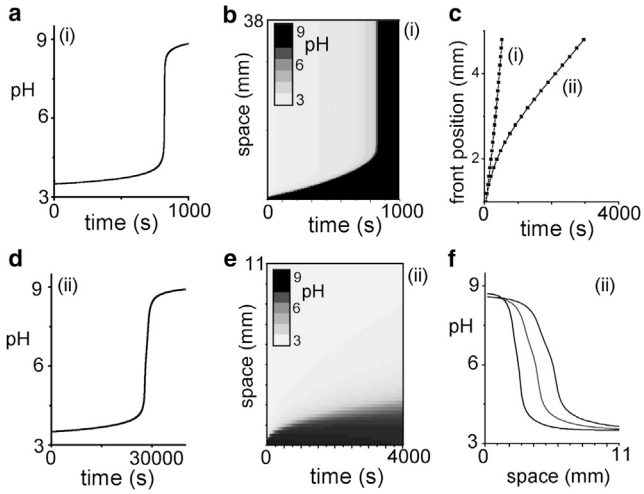

FIGURE 7 Simulated results for low enzyme: $[\text{urea}]_0 = 0.03$ M, [sulfuric acid]$_0 = 1.6 \times 10^{-4}$ M and (*i*) $[\text{urease}]_0 = 3.4$ unit/ml, (*ii*) $[\text{urease}]_0 = 0.1$ unit/mL. (*a* and *d*) pH-time plot in the well-stirred reaction. (*b* and *e*) Space-time plot in the 1D spatial reaction. (*c*) Front position in time. (*d*) pH-space profiles at 1000 s, 2500 s, and 4000 s.

0.1 U/ml (Fig. 7 *ii*), the spatial system supports fronts with the reacted solution at the first two grid points spreading diffusively initially and then propagating with constant pH-space profile and speed of the order of 0.057 mm min^{-1} (calculated from 3 to 5 mm) until the switch time.

DISCUSSION

Chemical fronts are driven by the reaction and diffusion of an autocatalytic species, and, in contrast to diffusion alone, have characteristic properties of concentration profiles in space that travel with constant amplitude and speed (30). We have demonstrated here that the spatially distributed urea-urease reaction supports pH wave fronts, converting the mixture from pH 3 to pH 9. The source of the feedback in the urea-urease reaction is the production of base, NH_3, coupled with the bell-shaped rate pH curve with a maximum at pH 7 (22). Thus, with the initial pH adjusted to pH 3 by addition of sulfuric acid, rate acceleration is expected as the reaction proceeds. Fronts are obtained in simulations with a Michaelis-Menten expression for enzyme activity, including a bell-shaped rate-pH dependence and diffusion of the basic product NH_3. The simplicity of this reaction makes it particularly useful for investigating the properties of traveling waves and stochastic effects driven by enzymatic feedback.

A number of inorganic reaction systems that support pH wave fronts, such as the bromate-sulfite (29) and chlorite-tetrathionate (31) systems, have been well investigated. Fronts speeds are usually of the order of 1–20 mm min^{-1} (provided that the front is not subject to convective effects), which is generally higher than the speeds observed here (0.1–1 mm min^{-1}). However, these well-studied systems involve reactions driven by acid autocatalysis, and little is known about fronts driven by base autocatalysis (32). In our experiments, the pH fronts have a constant intensity profile in space and the front position in time is best fit by a linear relationship. The simulations suggest that in fact, the fronts accelerate as the pH increases ahead of the front, a process that is enhanced by fast diffusion of H^+. This is more evident close to the switch time, where we typically do not take measurements experimentally due to noise. However, it may explain why the front speed at high enzyme, high urea, and low acid (i.e., short switch times) is higher than expected from the simulations.

In general, the front speed c may be related to the diffusion coefficient D of the autocatalyst and the reaction kinetics through the relation $c = (D/t)^{1/2}$, where t is the characteristic timescale of the reaction. A fit of a power relation of the form $y = Ax^B$ to the front speed-switch time plots resulted in exponents of the order of -0.5. However, the experimental fit is poor due to the significant degree of variability in front speed and switch time between runs. Aside from possible acceleration of the front during the course of the reaction, this is expected for two reasons: 1), enzyme activity may vary among samples; and 2), autocatalytic reactions are susceptible to fluctuations that may arise from imperfect mixing, resulting in variations in switch time (23).

The sensitivity of the reaction to the degree of mixing manifests in several ways. With enzyme concentrations >10 U/ml, there is an increase in the unstirred switch time relative to the stirred switch time. To obtain a similar magnitude of speed in simulations to experiments in the urea-urease reaction, we used an enzyme rate constant of 2.2×10^{-6} unit^{-1} ml M^{-1} s^{-1}, which is lower than that employed in our previous work in the well-stirred reactor (22). A prolonged switch time in the unstirred case is associated with consumption of an inhibitor in autocatalytic processes, and the dependence of the switch time on the stirring rate can be simulated with the use of micromixing models (33).

With lower enzyme concentrations of 3.4 U/ml, the reaction often failed to support pH fronts. It is surprising that the spatially distributed system did not support fronts when the well-stirred system still showed a switch to high pH in a few hundred seconds. This has not been observed in other autocatalytic reactions and may involve a loss of mass-action kinetics in the spatially distributed enzymatic system. One of the main differences between other pH autocatalytic systems and the urea-urease reaction is that the latter involves a catalyst, urease (22). For enzyme concentrations of 0.7 U/ml, we sometimes did not observe the switch in the well-stirred reaction. It would be of interest to determine the statistics associated with the probability of a pH front/switch being observed as the enzyme concentration is lowered from ~10 to 1 U/ml. It may be possible to reproduce these effects in a stochastic model (34).

CONCLUSION

We have demonstrated that the urea-urease reaction is one of a handful of enzyme reactions that show propagating chemical wave fronts in a single-phase system in vitro. The pH fronts are reproduced by a reaction-diffusion model with Michaelis-Menten kinetics containing a bell-shaped pH rate dependence. However, the model breaks down at low enzyme concentrations (<3 U/ml), and the unstirred system ceases to support pH fronts or switches even though the well-stirred reaction shows a rapid pH switch. The urease reaction is probably the simplest example of biochemical feedback and is therefore suitable for investigation of chemical waves and stochastic effects driven by enzymatic feedback. Pattern formation may be obtained if the reaction is performed in an open, unstirred reactor and coupled with an appropriate inhibitory reaction (35,36).

REFERENCES

1. Novák, B., and J. J. Tyson. 2008. Design principles of biochemical oscillators. *Nat. Rev. Mol. Cell Biol.* 9:981–991.
2. Miller, M. B., and B. L. Bassler. 2001. Quorum sensing in bacteria. *Annu. Rev. Microbiol.* 55:165–199.
3. Schütze, J., T. Mair, …, J. Wolf. 2011. Metabolic synchronization by traveling waves in yeast cell layers. *Biophys. J.* 100:809–813.
4. Gerisch, G., H. Fromm, …, U. Wick. 1975. Control of cell-contact sites by cyclic AMP pulses in differentiating *Dictyostelium* cells. *Nature.* 255:547–549.
5. Howard, J., S. W. Grill, and J. S. Bois. 2011. Turing's next steps: the mechanochemical basis of morphogenesis. *Nat. Rev. Mol. Cell Biol.* 12:392–398.
6. Gordon, P. V., C. Sample, …, S. Y. Shvartsman. 2011. Local kinetics of morphogen gradients. *Proc. Natl. Acad. Sci. USA.* 108:6157–6162.
7. Olsen, L. F., A. Z. Andersen, …, A. K. Poulsen. 2009. Regulation of glycolytic oscillations by mitochondrial and plasma membrane H^+-ATPases. *Biophys. J.* 96:3850–3861.
8. Beg, A. A., G. G. Ernstrom, …, E. M. Jorgensen. 2008. Protons act as a transmitter for muscle contraction in C. elegans. *Cell.* 132:149–160.
9. Monshausen, G. B., T. N. Bibikova, …, S. Gilroy. 2007. Oscillations in extracellular pH and reactive oxygen species modulate tip growth of *Arabidopsis* root hairs. *Proc. Natl. Acad. Sci. USA.* 104:20996–21001.
10. Stingl, K., K. Altendorf, and E. P. Bakker. 2002. Acid survival of *Helicobacter pylori*: how does urease activity trigger cytoplasmic pH homeostasis? *Trends Microbiol.* 10:70–74.
11. Amir, L., T. K. Tam, …, E. Katz. 2009. Biofuel cell controlled by enzyme logic systems. *J. Am. Chem. Soc.* 131:826–832.
12. Schreiber, I., Y. F. Hung, and J. Ross. 1996. Categorization of some oscillatory enzymatic reactions. *J. Phys. Chem.* 100:8556–8566.
13. Rabai, G., M. Orban, and I. R. Epstein. 1990. Systematic design of chemical oscillators. 64. Design of pH-regulated oscillators. *Acc. Chem. Res.* 23:258–263.
14. Elowitz, M. B., and S. Leibler. 2000. A synthetic oscillatory network of transcriptional regulators. *Nature.* 403:335–338.
15. Bagyan, S., T. Mair, …, S. C. Müller. 2005. Glycolytic oscillations and waves in an open spatial reactor: Impact of feedback regulation of phosphofructokinase. *Biophys. Chem.* 116:67–76.
16. Mair, T., and S. C. Müller. 1996. Traveling NADH and proton waves during oscillatory glycolysis in vitro. *J. Biol. Chem.* 271:627–630.
17. Bodó, G., R. M. M. Branca, …, C. Bagyinka. 2009. Concentration-dependent front velocity of the autocatalytic hydrogenase reaction. *Biophys. J.* 96:4976–4983.
18. Míguez, D. G., V. K. Vanag, and I. R. Epstein. 2007. Fronts and pulses in an enzymatic reaction catalyzed by glucose oxidase. *Proc. Natl. Acad. Sci. USA.* 104:6992–6997.
19. Caplan, S. R., A. Naparstek, and N. J. Zabusky. 1973. Chemical oscillations in membrane. *Nature.* 245:364–366.
20. Goldbeter, A., and S. R. Caplan. 1976. Oscillatory enzymes. *Annu. Rev. Biophys. Bioeng.* 5:449–476.
21. Vanag, V. K., D. G. Míguez, and I. R. Epstein. 2006. Designing an enzymatic oscillator: bistability and feedback controlled oscillations with glucose oxidase in a continuous flow stirred tank reactor. *J. Chem. Phys.* 125:194515.
22. Hu, G., J. A. Pojman, …, A. F. Taylor. 2010. Base-catalyzed feedback in the urea-urease reaction. *J. Phys. Chem. B.* 114:14059–14063.
23. Epstein, I. R. 1995. The consequences of imperfect mixing in autocatalytic chemical and biological systems. *Nature.* 374:321–327.
24. Chang, R. 2005. Physical Chemistry for the Biosciences. University Science Books, Sausalito, CA.
25. Krajewska, B., and S. Ciurli. 2005. Jack bean (*Canavalia ensiformis*) urease. Probing acid-base groups of the active site by pH variation. *Plant Physiol. Biochem.* 43:651–658.
26. Krajewska, B. 2009. Ureases I. Functional, catalytic and kinetic properties: A review. *J. Mol. Catal., B. Enzym.* 59:9–21.
27. Eigen, M. 1964. Proton transfer acid-base catalysis and enzymatic hydrolysis. 1. Elementary processes. *Angew. Chem. Int. Ed.* 3:1.
28. Ermentrout, G. B. 2002. Simulating, Analyzing, and Animating Dynamical Systems: A Guide to XPPAUT for Researchers and Students. SIAM, Philadelphia.
29. Keresztessy, A., I. P. Nagy, …, J. A. Pojman. 1995. Traveling waves in the iodate-sulfite and bromate-sulfite systems. *J. Phys. Chem.* 99:5379–5384.
30. Scott, S. K., and K. Showalter. 1992. Simple and complex propagation reaction diffusion fronts. *J. Phys. Chem.* 96:8702–8711.
31. Horvath, D., and A. Toth. 1998. Diffusion-driven front instabilities in the chlorite-tetrathionate reaction. *J. Chem. Phys.* 108:1447–1451.
32. Evans, R., C. R. Timmel, …, M. M. Britton. 2006. Magnetic resonance imaging of the manipulation of a chemical wave using an inhomogeneous magnetic field. *J. Am. Chem. Soc.* 128:7309–7314.
33. Strizhak, P., and M. Menzinger. 1996. Stirring effect on the bistability of the Belousov-Zhabotinsky reaction in a CSTR. *J. Phys. Chem.* 100:19182–19186.
34. Barik, D., M. R. Paul, …, J. J. Tyson. 2008. Stochastic simulation of enzyme-catalyzed reactions with disparate timescales. *Biophys. J.* 95:3563–3574.
35. Horváth, J., I. Szalai, and P. De Kepper. 2009. An experimental design method leading to chemical Turing patterns. *Science.* 324:772–775.
36. Gao, Q. Y., Y. L. Ana, and J. C. Wang. 2004. A transition from propagating fronts to target patterns in the hydrogen peroxide-sulfite-thiosulfate medium. *Phys. Chem. Chem. Phys.* 6:5389–5395.